

# Two-color magneto-optical trap with small magnetic field for ytterbium

Akio Kawasaki, Boris Braverman, QinQin Yu and Vladan Vuletic

Department of Physics, MIT-Harvard Center for Ultracold Atoms and Research Laboratory of Electronics, Massachusetts Institute of Technology, Cambridge, Massachusetts 02139, USA

E-mail: akiok@mit.edu

Received 22 March 2015, revised 9 May 2015

Accepted for publication 28 May 2015

Published 26 June 2015



CrossMark

## Abstract

We report a two-color magneto-optical trap (MOT) for ytterbium atoms where the slowing and trapping functions are separately performed by the singlet transition light ( $6s^2\ ^1S_0 \rightarrow 6s6p\ ^1P_1$ ) and the triplet transition light ( $6s^2\ ^1S_0 \rightarrow 6s6p\ ^3P_1$ ), respectively. The two-color MOT is achieved by simultaneously applying laser light on both the broad-linewidth singlet transition and the narrow-linewidth triplet transition. It is highly robust against laser power imbalance even at very low magnetic field gradients, and can operate at magnetic field gradients down to  $2\ \text{G cm}^{-1}$  where a conventional MOT using the singlet transition is unable to trap atoms. We load and trap up to  $4.0 \times 10^5$  atoms directly from an atomic beam at 700 K.

Keywords: magneto-optical trap, alkali earth-like atoms, laser cooling

## 1. Introduction

The magneto-optical trap (MOT) [1] has become the standard way of laser cooling and trapping neutral atoms. Due to its simplicity and robustness, the MOT has enabled many experiments with ultracold neutral atoms, such as quantum gases [2–4], cavity QED systems [5], and atomic clocks [6]. In a MOT, light slightly red-detuned from an atomic cycling transition provides cooling and trapping forces through the Doppler and Zeeman effects, respectively. In a conventional MOT for alkali atoms [1], both functions are performed by a single laser. However, the cooling and trapping can in principle be performed by light fields addressing two different transitions. At the cost of some technical complexity, the additional available parameters, such as transition linewidth, and laser intensity and detuning, may allow one to optimize the cooling and trapping functions separately, and improve the performance over the standard one-color MOT.

One class of atoms with two transitions of different linewidth are the alkaline earth and alkaline earth-like atoms. With two electrons in the outermost shell, these atoms have a broad-linewidth singlet transition and a narrow-linewidth triplet transition that are both suitable for a MOT. The broad singlet transition is excellent for slowing fast atoms, enabling their loading into a trap of finite depth. However, the singlet MOT has a minimum achievable Doppler temperature of

$\hbar\Gamma_s/(2k_B) \sim 1\ \text{mK}$ , set by the large transition linewidth of  $\Gamma_s/(2\pi) \simeq 30\ \text{MHz}$ . On the other hand, it requires a large magnetic field gradient of typically  $B' = 50\ \text{G cm}^{-1}$  [7–9] to match the Zeeman shift to  $\Gamma_s$  over a characteristic distance of 1 cm. The narrow triplet transition allows one to cool atoms down to temperatures of a few  $\mu\text{K}$ , corresponding to transition linewidths in the range of  $\Gamma_t/(2\pi) = (1 - 100)\ \text{kHz}$ , but the atoms have to be initially slow to be captured into a triplet MOT because the slowing force associated with the small scattering rate  $\leq \Gamma_t$  is too weak to capture fast atoms. Alkaline earth (-like) atoms have been cooled down to  $\mu\text{K}$  temperatures by applying light on the two transitions sequentially [10–19].

Among the alkaline earth-like atoms, ytterbium is widely used for the study of quantum gases [20, 21], atomic clocks [22], and quantum measurements [23]. As shown in figure 1(a), the  $6s^2\ ^1S_0 \rightarrow 6s6p\ ^1P_1$  transition (singlet transition) has a wavelength of  $\lambda_s = 399\ \text{nm}$  and a linewidth of  $\Gamma_s/(2\pi) = 28\ \text{MHz}$ . The  $6s^2\ ^1S_0 \rightarrow 6s6p\ ^3P_1$  transition (triplet transition) has a wavelength of  $\lambda_t = 556\ \text{nm}$  and a linewidth of  $\Gamma_t/(2\pi) = 184\ \text{kHz}$ .

Here, we report the realization of a two-color MOT (TCMOT) for ytterbium where 399 nm light and 556 nm light are simultaneously applied with complete spatial overlap. By separating the functions of cooling and trapping, the TCMOT can operate at a small magnetic field gradient  $B'$  where neither light on its own can cool and trap atoms efficiently. Our setup

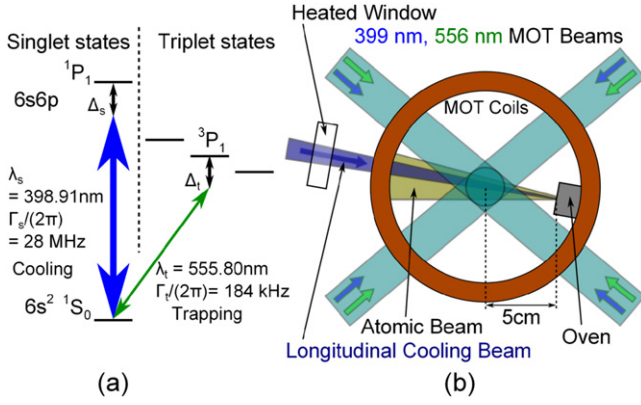


**Figure 1.** (a) Energy level diagram for ytterbium. We use the broad singlet transition (blue arrow) and narrow triplet transition (green arrow) for the TCMOT. (b) Schematic view of the experimental apparatus.

requires only  $B' = 5 \text{ G cm}^{-1}$  to trap a number of atoms similar to a conventional MOT operating on the singlet transition (singlet MOT) that uses a field gradient  $B'$  ten times larger, and is still robust down to  $B' = 2 \text{ G cm}^{-1}$ . Placing the atom source close to the MOT region enables us to operate the TCMOT without a Zeeman slower.

The TCMOT is most useful when electric power is limited, such as in portable or space-borne systems. In our case, the electric power necessary for the TCMOT was 40 times smaller than that for the singlet MOT with  $B' = 45 \text{ G cm}^{-1}$ . The electric power consumption in a 2D singlet MOT could also be substantially reduced with a 2D TCMOT. Furthermore, the TCMOT could be useful in situations where a small magnetic field is required to reduce the magnetization of materials around the atoms, e.g. in high-performance optical-transition clocks [22].

Experiments requiring the trapping and cooling of ytterbium down to  $\sim 5 \mu\text{K}$  in a MOT operated on the triplet transition (triplet MOT) have so far used one of the following three methods. The first method is to load the singlet MOT to trap a large number of atoms, and then transfer the atoms into a triplet MOT to cool them further [10–14]. This two-stage MOT is commonly used for other elements as well [15, 24–28]. The second method is to use a Zeeman slower to decelerate an atomic beam, allowing the atoms to be loaded directly into the triplet MOT [16–18]. The third method is to use a 2D singlet MOT to load a 3D triplet MOT [19]. All of these methods require high magnetic fields, because the singlet MOTs (both 2D and 3D) typically requires magnetic field gradients in the range of  $30\text{--}50 \text{ G cm}^{-1}$ , while a Zeeman slower requires a magnetic field on the order of 100 G.

Methods similar to ours, only in the sense that 399 nm and 556 nm light are applied simultaneously, have been very recently reported. Reference [29] describes the cooling of ytterbium atoms in an optical lattice by dual optical molasses, where 399 nm light and 556 nm light are sent simultaneously. In this method, the trapping force is provided by the optical lattice, and both 399 and 556 nm light are used only for the cooling. During the preparation of this manuscript, another

scheme for a small field gradient MOT was reported [30], where 556 nm light is sent in the central region, surrounded by a 399 nm light shell. In their system, the two lights do not have any spatial overlap. Therefore, in each region of their trap, both the cooling and the trapping functions are performed by a single light. This MOT is essentially a sequential MOT, where the singlet MOT is switched to the triplet MOT as the atoms move towards the center. The optimal magnetic field gradient in that experiment was close to ours,  $B' \simeq 5 \text{ G cm}^{-1}$ , but ours has better low field gradient performance; at  $B' = 2 \text{ G cm}^{-1}$ , TCMOT still has a quarter of the maximum atom number, but in [30], the loading rate drops roughly two orders of magnitude at  $B' = 2 \text{ G cm}^{-1}$  compared to  $B' = 5 \text{ G cm}^{-1}$ . In addition, the 556 nm light was spectrally broadened, and a Zeeman slower was used to increase the flux of slow atoms in [30].

## 2. Principle of the TCMOT

We can understand the TCMOT as an atom trap where the cooling and trapping functions are separately performed by two light fields. Each transition's contribution to the force on an atom in the trap at position  $z$  moving with velocity  $v$  is modeled simply as the sum of the forces  $F_{\pm}$  from counter-propagating beams with intensities  $I_{\pm}(z)$  [31]:

$$F_{\pm}(v, z) = \pm \frac{\hbar k \Gamma}{2} \frac{I_{\pm}(z)/I_{\text{sat}}}{1 + I_{\pm}(z)/I_{\text{sat}} + 4 \left( \frac{\Delta \pm kv \mp \mu B' z}{\Gamma} \right)^2} \quad (1)$$

with wavenumber  $k = 2\pi/\lambda$ , transition linewidth  $\Gamma$ , transition saturation intensity  $I_{\text{sat}}$ , detuning of the light from resonance  $\Delta$ , and magnetic moment associated with the transition  $\mu$ . The trap potential at position  $z$  for an atom at rest is calculated by numerically integrating this force along  $z$  direction.

$$U(z_0) = - \int_{-\infty}^{z_0} (F_+(0, z) + F_-(0, z)) dz \quad (2)$$

The maximum trap potential depth is obtained as the smaller value of  $|U(-\infty) - U(0)|$  and  $|U(\infty) - U(0)|$ .

Figure 2 shows the calculated slowing force for each of the transitions, and figure 3 shows the calculated trap potential depth for an atom at rest. According to figure 2, the broad singlet transition can address a substantially larger velocity range, and thus has a significantly larger contribution to slowing the atoms regardless of the field gradient  $B'$ . Note that the integrated flux in an atomic beam up to a capture velocity  $v_c$  scales as  $v_c^4$ . This means that for the conditions displayed in figure 2, the loading flux is 5000 times larger for the singlet light than for the triplet light. On the other hand, from figure 3, we see that at  $B' \lesssim 7 \text{ G cm}^{-1}$ , the trapping potential in the triplet MOT is deeper than in the singlet MOT, as the narrower triplet transition provides more frequency discrimination and thus a stronger magnetic-field-dependent restoring force. For the same reason, polarization impurities and intensity imbalance between two counter-propagating MOT beams has a larger effect on the singlet MOT than on the triplet MOT. As the intensity imbalance

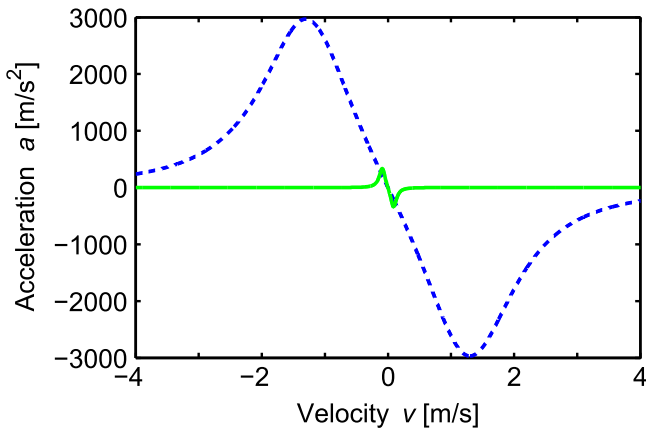


**Figure 2.** Calculated velocity dependence of the light-induced acceleration due to the singlet (blue dashed line) and triplet (green solid line) transitions. Parameters were set as  $\Delta_s = -0.7\Gamma_s$ ,  $\Delta_t = -5.5\Gamma_t$ ,  $I_s = 0.043I_{\text{sat},s}$ , and  $I_t = 27I_{\text{sat},t}$ .

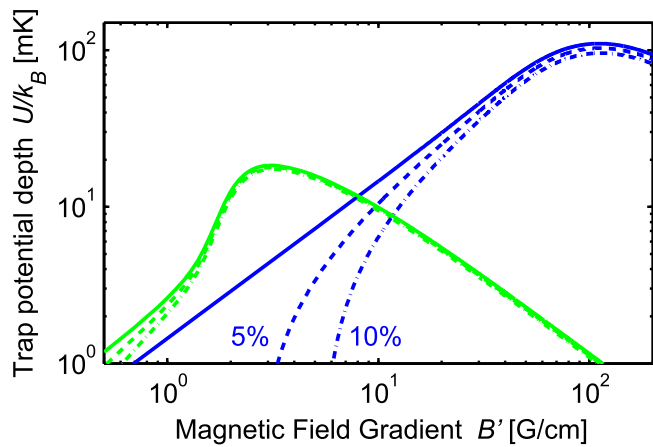


**Figure 3.** Calculated trapping potential depth for atoms at rest in the singlet MOT (blue lines) and the triplet MOT (green lines) versus  $B'$ : the solid lines, dashed lines, and dash-dotted lines are for an ideal MOT, and power imbalances of 5%, and 10% between the counter-propagating beams, respectively. Parameters were set as  $\Delta_s = -0.7\Gamma_s$ ,  $\Delta_t = -5.5\Gamma_t$ ,  $I_s = 0.043I_{\text{sat},s}$ ,  $I_t = 27I_{\text{sat},t}$ , and beam size 1 cm.

increases, the field gradient  $B'$  necessary to attain a certain trapping depth increases. We note that even for carefully balanced beams, reflections from various surfaces can easily give rise to interference that produces intensity variation of 5–10% across the beam profile.

By applying both the singlet transition and triplet transition light simultaneously, it is possible to produce a TCMOT that combines the large cooling force of the singlet transition with the deep trapping potential of the triplet transition at small field gradient  $B'$ . This is the main idea of our approach.

### 3. Experimental setup

Our apparatus is shown in figure 1(b). All trapping experiments are performed with  $^{174}\text{Yb}$  atoms, the isotope with the

largest natural abundance of 32%, though we also confirmed that  $^{171}\text{Yb}$  atoms are also trapped in TCMOT and atom number was comparable to that of  $^{174}\text{Yb}$  MOT. The frequency detunings of the lasers are measured from the  $^{174}\text{Yb}$  atomic resonances. Typically, the detunings for 399 nm and 556 nm light are  $\Delta_s = -0.7\Gamma_s$  and  $\Delta_t = -3.7\Gamma_t$ , respectively. The MOT beams have a  $1/e^2$  diameter of 1 cm. The total beam intensities, which is defined as the sum of the intensities of six MOT beams, for the 399 nm and 556 nm MOT beams are  $I_s = 0.26I_{\text{sat},s}$  and  $I_t = 160I_{\text{sat},t}$ , respectively, where  $I_{\text{sat},s} = 58 \text{ mW cm}^{-2}$  and  $I_{\text{sat},t} = 0.138 \text{ mW cm}^{-2}$  are the corresponding saturation intensities.

The atomic source is an oven heated up to 700 K, located 5 cm from the center of the MOT. In addition to the six MOT beams, we use a beam of 399 nm light, counterpropagating with respect to the atomic beam, in order to slow down a portion of the atomic beam. On the path of the slowing beam inside the vacuum chamber, a heated window at a temperature of 600 K with a power consumption of 12 W is placed in order to prevent the atomic beam from coating the vacuum chamber viewport. The slowing beam with a power of  $P_{\text{CP}} = 3 \text{ mW}$  is detuned by  $\Delta_{\text{CP}} = -4.6\Gamma_s$ . This beam is focused over a 65 cm distance from a 1.3 cm initial diameter to a tightest waist of  $13 \mu\text{m}$  at the collimating hole for the atomic beam.

The 399 nm light for the MOT and the slowing beam are produced by an external cavity diode laser system locked to the atomic transition by dichroic atomic vapor laser lock [32, 33], resulting in a laser linewidth of  $\sim 4 \text{ MHz}$ . The 556 nm light is produced by a frequency-doubled fiber laser that is locked to a reference cavity, with a short-term linewidth of 35 kHz.

We use two CCD cameras for atom number and atom cloud RMS radius measurements, and an avalanche photodiode for loading-time measurements. The typical measurement sequence consists of loading atoms into the TCMOT until the steady state, taking an image of the TCMOT, switching off the 399 nm light, and taking an image of the triplet MOT. Five measurements were averaged for each data point.

## 4. Experiments and interpretation

### 4.1. Properties of the TCMOT

We first compared the TCMOT with the singlet MOT. Figure 4(a) shows the dependence of atom number  $N$  on magnetic field gradient  $B'$  for the singlet MOT and the TCMOT. Our singlet MOT traps a maximum  $N = 4.0 \times 10^5$  at a relatively low  $B'$  of  $13.5 \text{ G cm}^{-1}$ , compared to a typical  $B'$  for a singlet MOT of  $30\text{--}45 \text{ G cm}^{-1}$  [7, 8]. This is likely due to careful adjustment of the retroreflection and the beam intensity balance, as well as the purity of the circular polarization. However, below  $13.5 \text{ G cm}^{-1}$ ,  $N$  quickly decreases to zero, and the singlet MOT vanishes altogether at  $6 \text{ G cm}^{-1}$ . This is consistent with a residual 5–10% beam intensity imbalance displayed in figure 3. On the other hand, the

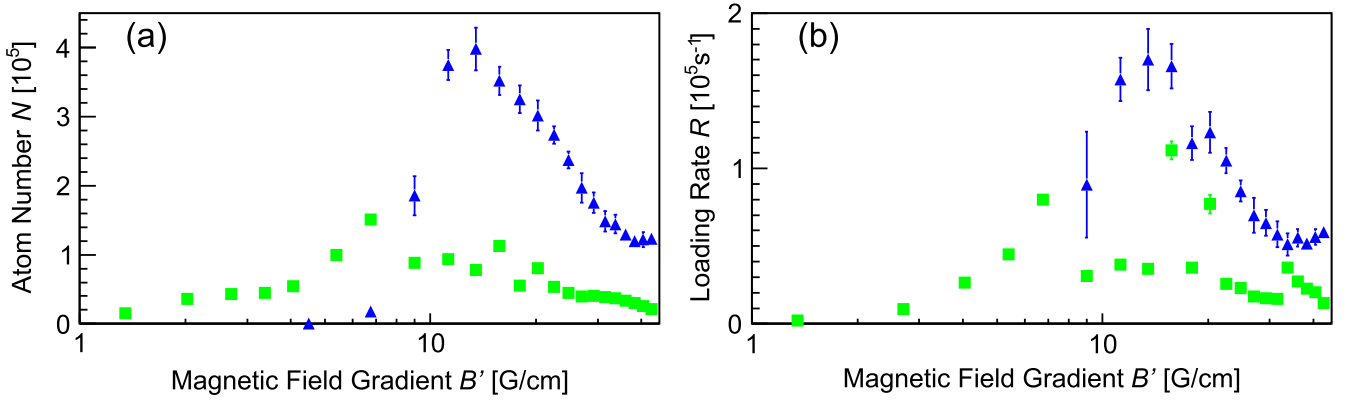


**Figure 4.** Comparison of the atom number (a) and the loading rate (b) in the singlet MOT (blue triangles) and the TCMOT (green squares) as a function of quadrupole field gradient  $B'$ : for  $B' \leq 6 \text{ G cm}^{-1}$ , the singlet MOT does not trap any atoms. Other parameters were  $\Delta_s = -0.7\Gamma_s$ ,  $\Delta_t = -3.7\Gamma_t$ ,  $I_s = 0.26I_{\text{sat},s}$ , and  $I_t = 160I_{\text{sat},t}$ . We believe that major source of the error bar is the frequency instability of 399 nm laser.

TCMOT still had  $N = 1.5 \times 10^5$  at  $6.75 \text{ G cm}^{-1}$ , comparable to the largest  $N$  for our singlet MOT. The somewhat smaller peak atom number for the TCMOT than for the singlet MOT is qualitatively explained by strong saturation of the triplet transition that results in a reduced scattering rate and slowing force on the singlet transition. The RMS radius of the singlet MOT is  $r_{\text{RMS}} = 2.1 \text{ mm}$ , compared to  $r_{\text{RMS}} = 0.7 \text{ mm}$  for the TCMOT. This factor of 3 in  $r_{\text{RMS}}$ , together with a factor of 8 in  $N$ , results in a  $\sim 200$  times larger atom density in the TCMOT at  $6.75 \text{ G cm}^{-1}$ . Figure 4(b) shows the loading rate of TCMOT is also comparable to that of the singlet MOT.

Figure 5 shows the atom number  $N$  and cloud size  $r_{\text{RMS}}$  of the TCMOT as a function of the detuning  $\Delta_s$ ,  $\Delta_t$  and the intensity  $I_s$ ,  $I_t$  of two lasers. Figure 5(a) shows the behavior of the TCMOT versus  $\Delta_s$ . The largest  $N$  is observed around  $\Delta_s = -0.7\Gamma_s$ . The TCMOT traps more atoms at large detuning  $|\Delta_s|$  compared to the singlet MOT. This is likely because for the singlet MOT the restoring force becomes too small at large detuning, while for the TCMOT the restoring force is provided by the 556 nm laser. Figure 5(b) shows the dependence of the atom number  $N$  on  $\Delta_t$ . The sharp increase of  $N$  near the resonance happens over a frequency range comparable to  $\Gamma_t$ , while the largest atom number is observed at  $\Delta_t = -22\Gamma_t$ . As a function of beam intensity, the atom number increases with  $I_s$  or  $I_t$ , until a plateau is observed at  $I_s \gtrsim 0.2I_{\text{sat},s}$ , and  $I_t \gtrsim 100I_{\text{sat},t}$ , as shown in figures 5(c) and (d).

When  $I_s = 0$ , we observe a pure triplet MOT with  $N = 1.9 \times 10^3$ , loaded directly from a thermal atomic beam (see figure 5(c)). With optimized parameters of  $\Delta_t = -14.7\Gamma_t$ ,  $\Delta_{\text{CP}} = -7.7\Gamma_s$ , and  $P_{\text{CP}} = 14 \text{ mW}$ , the atom number increased to  $(1.2 \pm 0.1) \times 10^4$ . Although this is four orders of magnitude smaller than the atom number reported in [16], to the best of our knowledge, this is the first observation of a triplet MOT being loaded from an atomic beam without a Zeeman slower or a 2D MOT.

For the TCMOT, with the optimized parameters  $B' = 6.75 \text{ G cm}^{-1}$ ,  $\Delta_t = -22\Gamma_t$ ,  $\Delta_s = -0.7\Gamma_s$ ,  $I_t > 100 I_{\text{sat},t}$ , and  $I_s > 0.20 I_{\text{sat},s}$ , we observe the largest atom number  $N = 4.0 \times 10^5$ . This is more than two orders of magnitude

smaller than the largest  $N$  reported in an ytterbium MOT [16, 30], primarily because our apparatus without Zeeman slower has been designed for cavity QED experiments that do not require a large number of atoms. Together with the oven temperature and the theoretically calculated capture velocity for the TCMOT of  $8 \text{ m s}^{-1}$ , the measured atomic beam flux  $2.2 \times 10^{10} \text{ s}^{-1}$  gives an estimated loading rate of  $6 \times 10^5 \text{ s}^{-1}$ , close to the best measured value of  $1 \times 10^5 \text{ s}^{-1}$ . Typical values for the atom flux, loading rate, and  $N$  with a Zeeman slower are  $10^{10} \text{ s}^{-1}$ ,  $10^7 \text{ s}^{-1}$ , and  $10^7$  for the singlet MOT [8, 34], and therefore, we would expect the TCMOT with a Zeeman slower to perform at least as well as a conventional singlet MOT with a Zeeman slower even with a conservative estimate.

The temperature for the TCMOT is 1 mK, slightly higher than the singlet transition Doppler limit of  $\hbar\Gamma_s/(2k_B) = 0.67 \mu\text{K}$ . This is 25 times larger than the expected temperature of  $\hbar\Delta_t/(2k_B) = 66 \mu\text{K}$  at  $\Delta_t = -3.7\Gamma_t$  [35] for the triplet MOT at the given detuning. This implies that the 556 nm light only traps the atoms but does not cool them down substantially in the presence of the scattering and the line broadening by the 399 nm light that heats the atoms toward the Doppler limit of the singlet transition.

#### 4.2. Experiments testing the model

To show the TCMOT relies on the simultaneous but independent effects from the singlet and the triplet light fields, we verified that when the two light fields are alternated sufficiently fast, the atom number is similar to that of the TCMOT at half the light intensity (table 1), while each laser alone traps a much smaller number of atoms.

To verify that the 556 nm light provides the dominant contribution to the trap confinement, we blocked the center of the 399 nm light with a 5.7 mm diameter disk (blocked TCMOT). We observe  $r_{\text{RMS}} = 0.67 \text{ mm}$  for the blocked TCMOT, quite close to  $r_{\text{RMS}}$  for the triplet MOT (table 1). This value, also close to  $r_{\text{RMS}} = 0.69 \text{ mm}$  observed for the TCMOT, shows that the singlet transition does not contribute significantly to the trapping. This method is similar to the

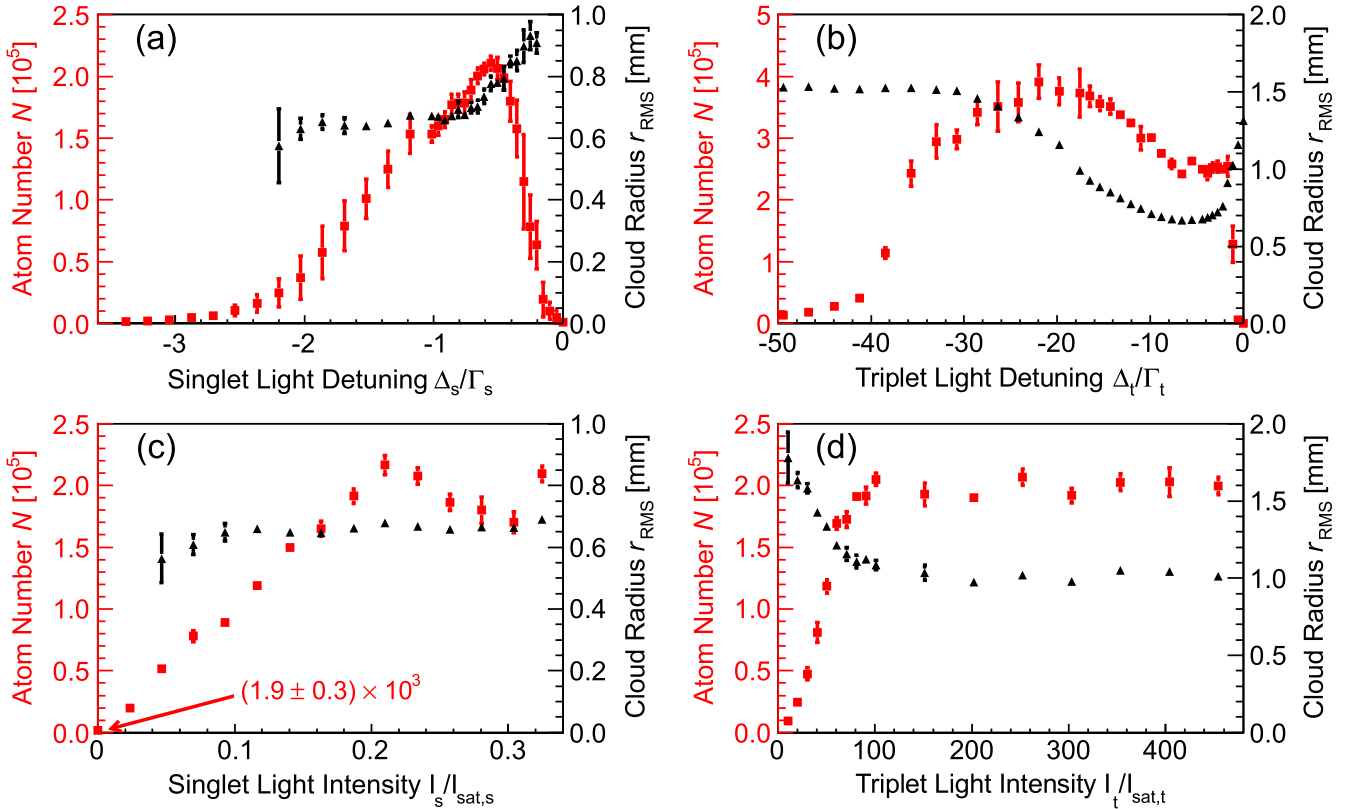


**Figure 5.** Characterization of the TCMOT: atom number  $N$  (red squares) and RMS cloud size  $r_{\text{RMS}}$  (black triangles) are plotted against (a)  $\Delta_s$ , (b)  $\Delta_t$ , (c)  $I_s$ , and (d)  $I_t$ . We varied only one parameter for each graph, shown on the horizontal axis. Fixed parameters were  $\Delta_s = -0.7\Gamma_s$ ,  $\Delta_t = -3.7\Gamma_t$ ,  $I_s = 0.26I_{\text{sat},s}$ ,  $I_t = 160I_{\text{sat},t}$ , and  $B' = 6.75 \text{ G cm}^{-1}$ . We believe that major source of the error bar is the frequency instability of 399 nm laser.

**Table 1.**  $N$  and  $r_{\text{RMS}}$  in the MOT in different conditions. Parameters are fixed at  $\Delta_s = -0.7\Gamma_s$ ,  $\Delta_t = -3.7\Gamma_t$ ,  $I_s = 0.26I_{\text{sat},s}$ ,  $I_t = 160I_{\text{sat},t}$ , and  $B' = 6.75 \text{ G cm}^{-1}$ . The errors shown are statistical errors; systematic errors are estimated to be 10%.

Condition	$N (\times 10^3)$	$r_{\text{RMS}}$ (mm)
Full power TCMOT	$243 \pm 10$	$0.69 \pm 0.01$
1/2 power TCMOT	$60 \pm 8$	$0.69 \pm 0.01$
25 kHz singlet/triplet switching	$25 \pm 3$	$0.80 \pm 0.09$
Pure singlet MOT	$5.4 \pm 0.7$	$2.04 \pm 0.03$
Pure triplet MOT	$1.1 \pm 0.2$	$0.61 \pm 0.02$
Blocked TCMOT	$16 \pm 1$	$0.67 \pm 0.01$

core-shell MOT described in [30], and the result is consistent with [30] in that adding 399 nm light to the triplet MOT enhances the atom number.

#### 4.3. Two-color MOT for other atomic species

The model described in section 2 predicts the range of ratios between the linewidths of the two transitions where the TCMOT is expected to work. The TCMOT requires that atoms cooled by the broad transition are cold enough to be confined by the narrow transition. The lower bound of the narrow transition linewidth for the TCMOT is  $k_B T_s \simeq U_t$ , where  $k_B T_s \sim \hbar \Gamma_s$  is the Doppler temperature of the singlet

MOT. The trap depth scales as  $U_t \sim \Gamma_t^{3/2}$ , as the force scales as  $\Gamma_t$  and the spatial range over which the transition is near resonant scales as  $\Gamma_t^{-1/2}$  because the saturation-broadened linewidth scales as  $\Gamma_t^{1/2}$ , assuming a constant laser intensity. This results in a lower bound of  $\Gamma_t/(2\pi)$  of 35 kHz for Yb, implying a maximum linewidth ratio of  $\Gamma_s/\Gamma_t \sim 800$ .

Hence we expect that the TCMOT could also be useful for cadmium [36], dysprosium [26, 37], erbium [27], and thulium [28, 38]. Cadmium trapping could especially benefit from the TCMOT, as in [36],  $B' = 500 \text{ G cm}^{-1}$  was used for the broad linewidth MOT. We note, however, that for cadmium, trapping by the narrow transition has not yet been observed, likely due to two photon ionization by the MOT light.

## 5. Conclusion

We have observed a TCMOT for ytterbium atoms where singlet and triplet transitions separately create the necessary cooling and trapping forces. By applying light on the singlet and triplet transitions simultaneously, MOT can be attained at low magnetic field gradients. The TCMOT trapped  $\sim 10^5$  atoms at  $B' = 5 \text{ G cm}^{-1}$ , displaying performance similar to a conventional singlet MOT at  $15 \leq B' \leq 45 \text{ G cm}^{-1}$ , and was robust down to  $B' = 2 \text{ G cm}^{-1}$ , where both conventional

singlet MOT and triplet MOT were unable to trap large a number of atoms. The atom number can be increased by means of a Zeeman slower, while the final temperature can be lowered by cooling only with 556 nm light at a reduced intensity after collecting the atoms [39]. The TCMOT could be beneficial in atom trapping experiments where a large magnetic field gradient is not permitted or desired.

## Acknowledgments

This research was supported by NSF and DARPA QuASAR. BB acknowledges support from the National Science and Engineering Research Council of Canada and QY from the Undergraduate Research Opportunity Program at MIT. We would like to thank Wolfgang Ketterle for insightful discussions.

## References

- [1] Raab E L, Prentiss M, Cable A, Chu S and Pritchard D E 1987 Trapping of neutral sodium atoms with radiation pressure *Phys. Rev. Lett.* **59** 2631–4
- [2] Anderson M H, Ensher J R, Matthews M R, Wieman C E and Cornell E A 1995 Observation of Bose–Einstein condensation in a dilute atomic vapor *Science* **269** 198–201
- [3] Davis K B, Mewes M O, Andrews M R, van Druten N J, Durfee D S, Kurn D M and Ketterle W 1995 Bose–Einstein condensation in a gas of sodium atoms *Phys. Rev. Lett.* **75** 3969–73
- [4] DeMarco B and Jin D S 1999 Onset of Fermi degeneracy in a trapped atomic gas *Science* **285** 1703–6
- [5] Miller R, Northup T E, Birnbaum K M, Boca A, Boozer A D and Kimble H J 2005 Trapped atoms in cavity qed: coupling quantized light and matter *J. Phys. B: At. Mol. Opt. Phys.* **38** S551
- [6] Ludlow A D, Boyd M M, Ye J, Peik E and Piet S O 2015 Optical atomic clocks arXiv:1407.3493
- [7] Park C Y and Yoon T H 2003 Efficient magneto-optical trapping of yb atoms with a violet laser diode *Phys. Rev. A* **68** 055401
- [8] Loftus T, Bochinski J R, Shivitz R and Mossberg T W 2000 Power-dependent loss from an ytterbium magneto-optic trap *Phys. Rev. A* **61** 051401
- [9] Honda K, Takahashi Y, Kuwamoto T, Fujimoto M, Toyoda K, Ishikawa K and Yabuzaki T 1999 Magneto-optical trapping of yb atoms and a limit on the branching ratio of the  $^1P_1$  state *Phys. Rev. A* **59** 934–7
- [10] Maruyama R, Wynar R H, Romalis M V, Andalkar A, Swallows M D, Pearson C E and Fortson E N 2003 Investigation of sub-doppler cooling in an ytterbium magneto-optical trap *Phys. Rev. A* **68** 011403
- [11] Kohno T, Yasuda M, Hosaka K, Inaba H, Nakajima Y and Hong F-L 2009 One-dimensional optical lattice clock with a fermionic  $^{171}\text{Yb}$  isotope *Appl. Phys. Express* **2** 072501
- [12] Park C Y *et al* 2013 Absolute frequency measurement of  $1s\ 0(f = 1/2)\ 3p\ 0(f = 1/2)$  transition of  $^{171}\text{Yb}$  atoms in a one-dimensional optical lattice at kriss *Metrologia* **50** 119
- [13] Lemke N D, Ludlow A D, Barber Z W, Fortier T M, Diddams S A, Jiang Y, Jefferts S R, Heavner T P, Parker T E and Oates C W 2009 Spin-1/2 optical lattice clock *Phys. Rev. Lett.* **103** 063001
- [14] Pandey K, Rathod K D, Singh A K and Natarajan V 2010 Atomic fountain of laser-cooled yb atoms for precision measurements *Phys. Rev. A* **82** 043429
- [15] Katori H, Ido T, Isoya Y and Kuwata-Gonokami M 1999 Magneto-optical trapping and cooling of strontium atoms down to the photon recoil temperature *Phys. Rev. Lett.* **82** 1116–9
- [16] Kuwamoto T, Honda K, Takahashi Y and Yabuzaki T 1999 Magneto-optical trapping of yb atoms using an intercombination transition *Phys. Rev. A* **60** 745–8
- [17] Ivanov V V, Khramov A, Hansen A H, Dowd W H, Münchow F, Jamison A O and Gupta S 2011 Sympathetic cooling in an optically trapped mixture of alkali and spin-singlet atoms *Phys. Rev. Lett.* **106** 153201
- [18] Peng-Yii Z, Zhuang-Xian X, Yun L, Ling-Xiang H and Bao-Long L 2009 Realization of green mot for ytterbium atoms *Chin. Phys. Lett.* **26** 083702
- [19] Dorschner S, Thobe A, Hundt B, Kochanek A, Targat R L, Windpassinger P, Becker C and Sengstock K 2013 Creation of quantum-degenerate gases of ytterbium in a compact 2d-/3d-magneto-optical trap setup *Rev. Sci. Instrum.* **84** 043109
- [20] Takasu Y, Maki K, Komori K, Takano T, Honda K, Kumakura M, Yabuzaki T and Takahashi Y 2003 Spin-singlet Bose–Einstein condensation of two-electron atoms *Phys. Rev. Lett.* **91** 040404
- [21] Fukuhara T, Takasu Y, Kumakura M and Takahashi Y 2007 Degenerate Fermi gases of ytterbium *Phys. Rev. Lett.* **98** 030401
- [22] Hinkley N, Sherman J A, Phillips N B, Schioppa M, Lemke N D, Beloy K, Pizzocaro M, Oates C W and Ludlow A D 2013 An atomic clock with  $10^{18}$  instability *Science* **341** 1215–8
- [23] Takano T, Fuyama M, Namiki R and Takahashi Y 2009 Spin squeezing of a cold atomic ensemble with the nuclear spin of one-half *Phys. Rev. Lett.* **102** 033601
- [24] Duarte P M, Hart R A, Hitchcock J M, Corcovilos T A, Yang T-L, Reed A and Hulet R G 2011 All-optical production of a lithium quantum gas using narrow-line laser cooling *Phys. Rev. A* **84** 061406
- [25] McKay D C, Jervis D, Fine D J, Simpson-Porco J W, Edge G J A and Thywissen J H 2011 Low-temperature high-density magneto-optical trapping of potassium using the open  $4s \rightarrow 5p$  transition at 405 nm *Phys. Rev. A* **84** 063420
- [26] Lu M, Burdick N Q, Youn S H and Lev B L 2011 Strongly dipolar Bose–Einstein condensate of dysprosium *Phys. Rev. Lett.* **107** 190401
- [27] Frisch A, Aikawa K, Mark M, Rietzler A, Schindler J, Zupanič E, Grimm R and Ferlaino F 2012 Narrow-line magneto-optical trap for erbium *Phys. Rev. A* **85** 051401
- [28] Sukachev D D, Kalganova E S, Sokolov A V, Fedorov S A, Vishnyakova G A, Akimov A V, Kolachevsky N N and Sorokin V N 2014 Secondary laser cooling and capturing of thulium atoms in traps *Quantum Electron.* **44** 515
- [29] Shibata K, Yamamoto R and Takahashi Y 2014 High-sensitivity *in situ* fluorescence imaging of ytterbium atoms in a two-dimensional optical lattice with dual optical molasses *J. Phys. Soc. Japan* **83** 014301
- [30] Lee J, Lee J H, Noh J and Mun J 2015 Core-shell magneto-optical trap for alkaline-earth-metal-like atoms *Phys. Rev. A* **91** 053405
- [31] Loftus T H, Ido T, Boyd M M, Ludlow A D and Ye J 2004 Narrow line cooling and momentum-space crystals *Phys. Rev. A* **70** 063413
- [32] Corwin K L, Lu Z-T, Hand C F, Epstein R J and Wieman C E 1998 Frequency-stabilized diode laser with the zeeman shift in an atomic vapor *Appl. Opt.* **37** 3295–8

- [33] Kim J I, Park C Y, Yeom J Y, Kim E B and Yoon T H 2003 Frequency-stabilized high-power violet laser diode with an ytterbium hollow-cathode lamp *Opt. Lett.* **28** 245–7
- [34] Cho J W, Lee H-G, Lee S, Ahn J, Lee W-K, Yu D-H, Lee S K and Park C Y 2012 Optical repumping of triplet-p states enhances magneto-optical trapping of ytterbium atoms *Phys. Rev. A* **85** 035401
- [35] Lett P D, Phillips W D, Rolston S L, Tanner C E, Watts R N and Westbrook C I 1989 Optical molasses *J. Opt. Soc. Am. B* **6** 2084–107
- [36] Brickman K-A, Chang M-S, Acton M, Chew A, Matsukevich D, Haljan P C, Bagnato V S and Monroe C 2007 Magneto-optical trapping of cadmium *Phys. Rev. A* **76** 043411
- [37] Youn S H, Lu M, Ray U and Lev B L 2010 Dysprosium magneto-optical traps *Phys. Rev. A* **82** 043425
- [38] McClelland J J and Hanssen J L 2006 Laser cooling without repumping: a magneto-optical trap for erbium atoms *Phys. Rev. Lett.* **96** 143005
- [39] Hansen A H, Khramov A Y, Dowd W H, Jamison A O, Plotkin-Swing B, Roy R J and Gupta S 2013 Production of quantum-degenerate mixtures of ytterbium and lithium with controllable interspecies overlap *Phys. Rev. A* **87** 013615